TU Delft

Delft University of Technology

Evaluation of membrane fouling at constant flux and constant transmembrane pressure conditions

Implications for membrane modification

Chen, Mingliang; Rietveld, Luuk C.; Heijman, Sebastiaan G.J.

DOI
10.1016/j.jece.2025.117823

Publication date
2025

Document Version
Final published version

Published in
Journal of Environmental Chemical Engineering

Citation (APA)
Chen, M., Rietveld, L. C., & Heijman, S. G. J. (2025). Evaluation of membrane fouling at constant flux and constant transmembrane pressure conditions: Implications for membrane modification. *Journal of Environmental Chemical Engineering*, *13*(5), Article 117823. https://doi.org/10.1016/j.jece.2025.117823

Important note
To cite this publication, please use the final published version (if applicable).
Please check the document version above.

Copyright
Other than for strictly personal use, it is not permitted to download, forward or distribute the text or part of it, without the consent of the author(s) and/or copyright holder(s), unless the work is under an open content license such as Creative Commons.

Takedown policy
Please contact us and provide details if you believe this document breaches copyrights.
We will remove access to the work immediately and investigate your claim.

This work is downloaded from Delft University of Technology.
For technical reasons the number of authors shown on this cover page is limited to a maximum of 10.

Journal of Environmental Chemical Engineering 13 (2025) 117823

Contents lists available at ScienceDirect

Journal of Environmental Chemical Engineering

journal homepage: www.elsevier.com/locate/jece

Evaluation of membrane fouling at constant flux and constant transmembrane pressure conditions: Implications for membrane modification

Mingliang Chen *, Luuk C. Rietveld, Sebastiaan G.J. Heijman

Sanitary Engineering, Department of Water Management, Faculty of Civil Engineering and Geosciences, Delft University of Technology, Stevinweg 1, Delft 2628 CN, the Netherlands

ARTICLE INFO

Keywords:
Constant flux filtration
Constant transmembrane pressure filtration
Threshold flux
Oil-in-water emulsion
Membrane fouling
Membrane modification

ABSTRACT

Membrane modification is commonly applied in water purification and wastewater treatment to reduce fouling of membranes. However, the influence of fouling test methods on evaluating pristine and modified membranes is often overlooked. This study investigates fouling behavior of alumina and SiC-deposited alumina membranes during oil-in-water emulsion filtration under both constant flux and constant transmembrane pressure conditions. Threshold flux was first determined using flux-stepping experiments, with the 90-min SiC-deposited membrane showing the highest value at 95 L m^{-2} h^{-1}. In single-cycle constant flux tests, fouling trends aligned with threshold flux data. However, when backwash was included, fouling characteristics shifted and depended on the permeate flux. Enhanced hydrophilicity and surface charge improved backwash efficiency in modified membranes. Yet, extensive modification negatively affected performance due to significant permeance loss (>57 %). Under constant pressure, fouling was dominated by internal pore blocking, and backwash efficiency was solely linked to membrane permeance, regardless of surface properties. Thus, constant flux filtration with backwash best reflects operational conditions and is recommended for evaluating membrane modifications.

1. Introduction

Among the membrane technologies, microfiltration (MF)/ultrafiltration (UF) are widely used for drinking water production [1,2], wastewater treatment [3,4] and pretreatment for high-pressure nanofiltration (NF) and reverse osmosis (RO) processes [5,6], due to their low energy requirement and small footprint. In addition, MF/UF are also considered to be one of the most effective ways to deal with oil-in-water (O/W) emulsions [7–15].

The filtration mechanism for MF/UF is mainly based on size exclusion [16]. During the filtration process, suspended particles, colloids and oil droplets are retained on the membrane surface or in the pores. This leads to the membrane fouling, which could cause a series of negative effects such as a decline of water production or a higher operational pressure due to an increased mass-transfer resistance [17]. As a result, the capital and operational costs increase due to higher energy consumption, requiring chemical cleaning of the fouled membranes and shorter membrane unit's service life. It is therefore important to mitigate membrane fouling during the filtration process.

Various techniques may be used to alleviate membrane fouling. The feed may be pre-treated by dosing additives (e.g., coagulant and flocculant) or oxidants (e.g., permanganate, chlorine) to reduce the amount of foulants that may block the membrane pores [18–20]. However, this can increase the operational costs due to the need of additional unit operations. Operational parameters, such as cross-flow velocity, permeate flux, and transmembrane pressure (TMP) can be adjusted to reduce foulant build-up on the membrane surface, but it cannot solve the fouling problem [17].

Membrane modification is considered to be one of the most promising methods to reduce membrane fouling [8]. This is normally achieved by building a fouling resistant surface on the membrane support. Various methods, such as surface coating [21,22], surface grafting [23], physical doping/blending [24] and surface deposition [7,25], have been adopted to construct such surfaces. The newly constructed surface can change the physicochemical properties of the membrane to minimize the negative interaction between the foulants and membrane surface, thereby decreasing fouling. This is typically realized via enhancing the surface hydrophilicity and electrostatic interactions between the

* Corresponding author.
E-mail address: mlchen620@gmail.com (M. Chen).

https://doi.org/10.1016/j.jece.2025.117823
Received 7 April 2025; Received in revised form 28 June 2025; Accepted 30 June 2025
Available online 1 July 2025
2213-3437/© 2025 The Author(s). Published by Elsevier Ltd. This is an open access article under the CC BY license (http://creativecommons.org/licenses/by/4.0/).

foulants and membranes in light of the fact that most of the foulants in nature are hydrophobic and charged in the aquatic environment [26].

Nevertheless, a higher mass-transfer resistance is commonly observed in MF/UF membranes after modification, due to either a decrease in membrane pore sizes or an increase in the selective layer thickness of the membrane. Therefore, the permeance of the modified membranes is usually smaller than that of the pristine membranes [27]. To effectively evaluate the extent of fouling mitigation for a modified membrane, the fouling rate during filtration and the fouling state after cleaning should be determined. There are two different filtration modes, namely constant TMP filtration and constant flux filtration (Fig. 1). Constant TMP filtration is more frequently used in a laboratory environment as it is relatively easy to perform. With a fixed TMP, the permeate flux of the membrane declines as it fouls. In contrast, constant flux filtration is preferred in industrial practice to maintain a constant production flow. To maintain the desired permeate flux, the TMP increases over time as the membrane fouls.

As the permeance is different for the modified and pristine membranes, fouling on the membrane surface or in the pores may be affected. As schematically shown in Fig. 1, due to the smaller permeance, the initial TMP and flux of the modified membrane are, respectively, higher and lower than that of the pristine membrane in constant flux mode and constant TMP mode [28,29]. As fouling is affected by the initial states, the higher initial flux through a pristine membrane may lead to more fouling in constant TMP mode [28]. Differences in the flux of filtration naturally occur for membranes with different permeances, making a fair comparison difficult. In comparison, in constant flux filtration mode, the higher initial TMP of the modified membrane also has a negative effect on fouling, making the comparison beneficial for membranes with a higher permeance [30].

Therefore, in both filtration modes, membrane fouling is affected by the variations of initial states of the membranes with different permeance. In a previous study, Miller et al. [29] compared the fouling of polymeric membranes at, respectively, constant TMP and constant flux modes for O/W emulsions. Mass-transfer resistance changes during fouling were compared at various fluxes for the two filtration modes. At low fluxes, the fouling resistance and its change were independent of the operational mode. In contrast, the change in fouling resistance was much higher in constant flux filtration than in constant TMP filtration experiments at high flux conditions. Although it was confirmed that membrane fouling could be affected by filtration modes, the effect of membrane permeance and the irreversible fouling (fouling that cannot be removed by physical or hydraulic cleaning) was not considered. More recently, Blankert et al. [28] also compared the fouling of membranes with different permeance at the two operational modes. The results showed that a bias may occur for a less-permeable membrane in constant TMP filtration mode due to a lower filtration flux. Hence, constant flux filtration experiments were recommended for fouling evaluation. However, the study focused solely on single-cycle filtration and did not consider the impact of irreversible fouling, despite its known role in increasing energy consumption and operational costs in full-scale setups [31,32]. Any modifications made could potentially influence membrane performance, particularly the irreversible fouling due to the newly formed functional layer. The combination of both factors (the decrease of permeance and the potential decrease of fouling by the newly formed selective layer) will finally determine the performance of a modified membrane.

To systematically evaluate membrane performance before and after surface modification under both constant flux and constant TMP filtration modes, we selected alumina membranes with and without a silicon carbide (SiC) coating. The membranes were challenged with an O/W emulsion. Oily wastewater is considered more challenging to treat than other types of wastewaters due to the complex composition of its water matrix, which includes surfactants, organic pollutants, ions, and suspended solids [33]. The hydrophobic nature of oil droplets causes them to readily adsorb onto polymeric membrane surfaces, leading to fouling and reduced efficiency [34,35]. As a result, ceramic membranes are often preferred for oily wastewater treatment because of their inherent hydrophilicity and higher resistance to fouling [36,37]. Among ceramic membranes, SiC membranes are reported to exhibit superior fouling resistance during O/W emulsion separation [38–40]. This enhanced performance is attributed primarily to the abundance of hydroxyl groups on the SiC surface, which confer strong hydrophilicity. Furthermore, SiC possesses a low isoelectric point (pH 2–3), resulting in a highly negatively charged surface [41,42]. These properties are crucial to alleviate membrane fouling during filtration of O/W emulsions.

In our previous work, we have developed a low-pressure chemical vapor deposition (LPCVD) technique for SiC layer deposition onto Al_2O_3 membrane surfaces and within their pores, thereby altering their properties and permeance [25]. Varying deposition times yielded membranes with different permeance levels. The novelty of this study lies in the comprehensive evaluation of membrane performance under both constant flux and constant TMP filtration modes. Specifically, threshold fluxes—defined as the flux values beyond which membrane fouling rates sharply increase—were first determined for each membrane type. Subsequently, membrane fouling behavior was systematically investigated under operating conditions both below and above these threshold fluxes in constant flux filtration mode. Additionally, by maintaining equal driving forces at two different TMPs and comparing membranes with equal initial fluxes but different driving forces, the study eliminated the impact of varying initial filtration fluxes. Finally, the fouling mechanisms of the membranes were respectively identified for constant TMP and constant flux filtration experiments.

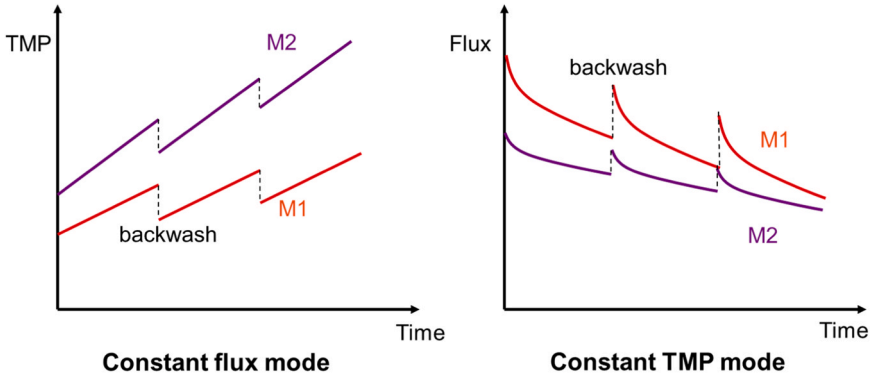

Fig. 1. Possible filtration profiles of the pristine membrane (M1) and the modified membrane (M2) at constant flux (left) and constant TMP (right) conditions.

2. Materials and methods

2.1. Materials

Mineral oil (330760), and sodium dodecyl sulphate (SDS) (> 99 %) were ordered from Sigma-Aldrich. Sodium chloride (NaCl) (99 %, Baker Analyzed) and citric acid (99.9 %, powder) were ordered from VWR. NaOH (0.1 M) was ordered from Merck. All chemicals and solvents were used as received without further purification. Demineralized water (produced by a reverse osmosis filter, a candle filter and a resin vessel), was used to prepare the aqueous solution and to rinse the filtration system and membrane samples.

2.2. Ceramic membranes

Commercial Al_2O_3 membranes (CoorsTek, the Netherlands) were used as supports for LPCVD deposition. These membranes have a nominal pore size of 100 nm with an inner and outer diameter of 7 mm and 10 mm, and a length of 150 mm. The LPCVD process was conducted at Else Kooi Lab, TU Delft. The details of the LCPVD equipment and deposition parameters have been given in our previous work [25]. In brief, a thin SiC layer was deposited onto the inner surface of the Al_2O_3 tubes using dichlorosilane (SiH_2Cl_2) and a C_2H_2/H_2 gas mixture as precursors, at a deposition temperature of 750 °C and a pressure of 80 Pa. To produce SiC-coated membranes with varying permeance, the layer thickness was controlled by adjusting the deposition time. Three different deposition times (60, 90 and 120 min) were chosen to obtain the SiC-deposited membranes with varying permeance, as detailed in Table 1. For simplicity, the membranes are referred to as D0, D60, D90, and D120, corresponding to their respective deposition times.

2.3. Membrane characterization

Zeta potential measurements were performed to characterize the surface charge of the membranes using a SurPASS electrokinetic analyzer (Anton Paar, Graz, Austria). The instrument operates by measuring the streaming potential across the membrane surface, and the corresponding zeta potential is calculated using the Helmholtz–Smoluchowski equation [43]. A 1 mM solution of potassium chloride (KCl) served as the electrolyte. All measurements were carried out at the same pH as that of the O/W emulsion to ensure consistency with the filtration conditions.

The water contact angles of the membranes were measured by a contact angle measurement machine (Dataphysics OCA20, Germany). Atomic force microscopy (AFM) (Dimension Icon, Bruker, USA) was used to determine the surface roughness of the membranes.

2.4. Oil-in-water emulsion

O/W emulsions were prepared by mixing mineral oil, SDS and NaCl in demineralized water. To make sure that the feed characteristics were consistent for each experiment, a stock emulsion was prepared with the following steps. First, 0.053 g NaCl was added in 0.9 L demineralized water and stirred for 10 min, afterwards, 0.9 g SDS was added to the NaCl solution. When SDS was totally dissolved, 4.5 mL mineral oil was added and continuously stirred with a magnetic stirrer (L23, LABINCO, the Netherlands) at a speed of 1500 rpm for 24 h. To improve emulsification and homogenization, the O/W mixture was further treated with an energy-intensive sonifier (Branson 450) at an intensity of 40 % for 30 min.

The stock emulsion was diluted 10 times in 1 mM NaCl solution to obtain a final oil concentration of 400 mg L^{-1}, SDS of 100 mg L^{-1} and NaCl of 1 mM for filtration experiments. Each filtration run was finished on the same day to reduce the effect of oil droplet aggregates or coalescence. The pH and conductivity of the emulsions were 5.6 and 156 μs/cm, as measured by a multi-meter sensor (inoLab™ Multi 9420 - WTW). The emulsion has an oil droplet size distribution in a range 1–10 μm (Fig. S1) and zeta potential of −90 mV, which were analyzed with a particle size analyzer (Bluewave, Microtrac, USA) and a Malvern Zetasizer Nano ZS (Malvern Instruments Ltd., UK), respectively.

2.5. Fouling experiments with O/W emulsions

2.5.1. Constant flux crossflow fouling experiments

The fouling of the membranes was first tested using a constant flux crossflow fouling apparatus, as detailed in Chen et al. [25]. The effective filtration area of each membrane module was 0.003 m^2. A constant permeate flux was maintained using a diaphragm pump (DDA12–10, Grundfos, Denmark) installed on the feed side. To ensure consistent hydrodynamic conditions, a crossflow velocity of 0.44 m s^{-1} was applied using a circulation pump (VerderGear, Verder B.V., The Netherlands), as established in our previous study [25]. During the filtration, the concentrate valve was closed and the oil concentration in the closed loop (150 mL) gradually increased with filtration time (e.g., 120 mL permeate was produced in 30 min at a flux of 80 L m^{-2} h^{-1}). Two pressure transducers (GS4200-USB, ESI, UK) were installed on the two sides of the membrane module to monitor the TMP during filtration process. The TMP increased with time due to membrane fouling and increased mass transfer resistance.

The filtration experiments were conducted at room temperature (22 ± 3 °C). The system was first cleaned with water to remove any residual chemical and air before loading the membrane module. The initial permeance of the membrane was determined with water at the same permeate fluxes as used for O/W filtration. Prior to formal fouling experiments, the threshold flux of each membrane was first determined by the flux stepping experiments as recommended in literature [44–46]. In this protocol, the membrane was initially operated at a low, constant flux of 40 L m^{-2} h^{-1} for 10 min. The flux was then incrementally increased by 10 L m^{-2} h^{-1} every 10 min. This stepwise increase continued until reaching a final flux of 110 L m^{-2} h^{-1}, at which point a sharp rise in fouling was observed, indicating the onset of rapid membrane fouling. Between each flux step, the membrane was backwashed at 3 bar for 15 s to remove the possible accumulated fouling from the previous flux step. To check if backwash affects the fouling character, the membranes were respectively tested with a single-cycle filtration at fluxes below and above the threshold flux and multi-cycle filtration with backwash, at three permeate fluxes (Table 2).

In single-cycle filtration, the experiments were extended for a longer period compared with the multi-cycle filtration experiments to differentiate the fouling between membranes. For multi-cycle filtration, the fouling experiment for each membrane consisted of six cycles. Each filtration cycle included three sequential phases: 1) Filtration at a specified flux for a pre-set time (Table 2), 2) Hydraulically reversible

Table 1
Characteristics of the Al_2O_3 membranes before and after SiC deposition.

Membrane label	Deposition time (min)	Selective layer	Pore size[a] (nm)	Membrane Resistance (× 10^{11} m^{-1})	Permeance (L m^{-2} h^{-1} bar^{-1})
D0	0	α-Al_2O_3	71	10	350 ± 10
D60	60	SiC	60	14	250 ± 15
D90	90	SiC	54	18	200 ± 20
D120	120	SiC	47	24	150 ± 10

[a] - the data is from Chen et al. [7].

Table 2
Permeate flux and the corresponding filtration time per cycle for constant flux multi-cycle filtration experiments.

Flux (L m^{-2} h^{-1})	80	90	100
Time (min)	30	20	18

fouling cleaning by backwashing the membrane module at a fixed pressure of 3 bar for 15 s using demineralized water, 3) Forward flush the system with feed emulsion for 15 s to clear residual liquids.

2.5.2. Constant TMP crossflow fouling experiments

Constant TMP crossflow fouling experiments were performed with a setup shown in Fig. 2. Unlike the constant flux experiment, only one pump (VerderGear, Verder B.V., the Netherlands) was used to pump the feed solution through the membrane module. The feed flow rate was monitored using a flow meter (Zhongjiangenergy-efficient electronics co., Itd., China) and a same crossflow velocity (0.44 m s^{-1}) was used as in the constant flux experiment. Two pressure transducers from ESI (GS4200-USB, UK) were used to monitor the pressures on two sides of the membranes. The TMP and crossflow velocity of the system were adjusted by controlling the speed of feed pump and a pressure control valve (FDV30KTZ, KNF) (downstream of the membrane module) simultaneously. In addition, a backwash vessel filled with demineralized water was installed at the permeate side. A fixed pressure of 3 bar was used to remove hydraulic reversible fouling of the membrane for 15 s.

Permeate from the membrane module was collected in a beaker on a digital balance (FZ-3000iWP, A&D company). The change in mass was automatically recorded every 30 s to the computer and therefore the permeate flux of the membrane was calculated by the following Eq. (1):

$$J = \frac{\Delta M}{\rho A \Delta t} \quad (1)$$

Where J is the flux (L m^{-2} h^{-1}), ΔM is the mass of permeate during a filtration period of Δt, ρ is the density of permeate and A is the effective filtration area of the membrane (0.003 m^2).

To begin a constant TMP fouling experiment, the membrane was first tested with demineralized water for 10 min to get a stable permeate flux at the setting pressures. Afterwards, the feed line was switched to the O/W emulsion to initialize the fouling experiment.

The fouling experiments in constant TMP mode were executed in two ways. First, all membranes were respectively compared at the same driving forces of 0.5 bar and 1 bar for three cycles. Each cycle lasted 20 min. In this case, the permeate flux was lower for the less permeable membranes. Afterwards, fouling experiments with different driving forces were adopted to obtain similar initial fluxes for all membranes (Table S1). These experiments consisted of six cycles with a duration of 20 min each.

2.6. Membrane cleaning

Following each fouling experiment, the membranes were chemically cleaned using a sequential treatment with a 0.01 M sodium hydroxide (NaOH) solution and a 0.01 M citric acid solution, each applied at 65 °C for 1 h, as described in previous studies [47,48]. Between these cleaning steps, the membranes were rinsed with demineralized water three times to remove residual chemicals. If chemical cleaning alone did not fully restore membrane performance, an additional thermal regeneration step was carried out by heating the membrane at 200 °C for 2 h in a muffle furnace (Nabertherm Controller P 300, Germany).

2.7. Data analysis

Normalized TMP, permeance and flux were employed to make the comparison between the different membranes possible, as variations in the initial pressure and flux existed among the membranes with varying permeance. The permeance recovery (R_p) of the membrane after backwash was calculated using Eq. (2):

$$R_p = P_i/P_0 \quad (2)$$

where P_i (L m^{-2} h^{-1} bar^{-1}) is the initial permeance of the membrane after i^{th} backwash cleaning, P_0 (L m^{-2} h^{-1} bar^{-1}) is the initial permeance of the clean membrane.

The oil concentration of the samples was measured by a UV/Vis spectrophotometer (GENESYS 10S UV-Vis, Thermo scientifical, US) at 275 nm. The membrane rejection was determined as follows:

$$R = (1 - C_p/C_f) \times 100\% \quad (3)$$

where R is the membrane rejection, C_p (mg/L) is the oil concentration in the permeate and C_f (mg/L) is the oil concentration in the feed.

In addition, the fouling of the membrane was analysed using the unified membrane fouling index (*UMFI* (m^2/L)), as described in Eq. (4). A detailed description of the *UMFI* can be found in a previous work [49].

$$\frac{1}{J_s} = 1 + (UMFI) \times V_s \quad (4)$$

where J_s' represents the normalized specific permeate flux and V_s (L/m^2) is the unit permeate volume. A higher UMFI value means a higher fouling rate present in a membrane during filtration of an O/W emulsion.

2.8. Membrane fouling analysis

To investigate the fouling mechanisms of membranes caused by oil droplets, various fouling models were employed in both constant TMP and constant flux filtration experiments. Specifically, for constant TMP crossflow filtration, the widely accepted model developed by Field et al. [50], as detailed in Eq. (5), was utilized. Note that this model was

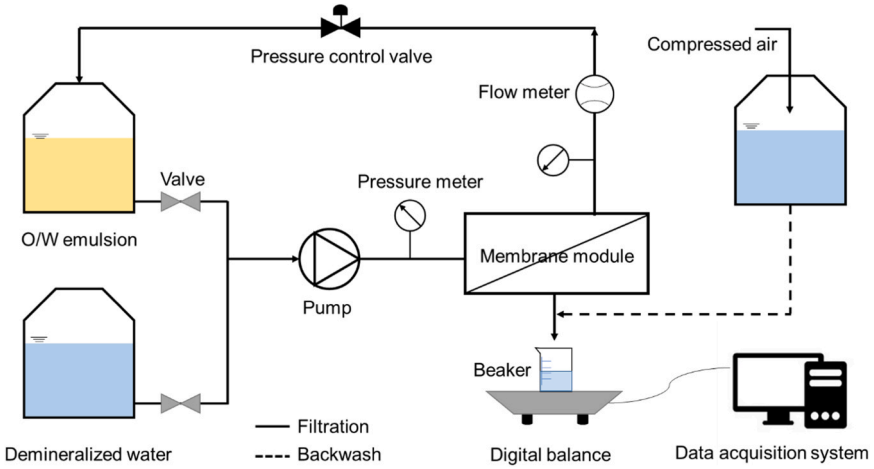

Fig. 2. Constant TMP crossflow filtration setup for O/W emulsion separation integrated with backwash.

developed for non-deformable spherical particles that are large enough with negligible back diffusion.

$$\frac{dJ}{dt} = -k(J-J^*)J^{n-2} \tag{5}$$

where J (m/s) is the permeate flux of the membrane, J^* is the critical flux of the membrane, k is fouling constant, n is the index and t is the filtration time (s).

According to Hermia's theory, the fouling mechanism of the membrane can be classified into complete pore blocking (n = 2), standard pore blocking (n = 1.5), intermediate pore blocking (n = 1) and cake filtration (n = 0). By substituting the n value into Eq. (4) and rearranging, we can derive the following four equations:

Complete pore blocking (n = 2):

$$J = J^* + (J_0 - J^*) \times e^{(-k_c t)} \tag{6}$$

Standard pore blocking (n = 1.5):

$$J = \frac{1}{(\frac{1}{\sqrt{J_0}} + k_s t)^2} \tag{7}$$

Intermediate pore blocking (n = 1):

$$J = J^* \Big/ [1 - \frac{(J_0 - J^*)}{J_0} \times \exp(-J^* k_i t)] \tag{8}$$

Cake filtration (n = 0):

$$k_l t = 1 \Big/ J^{*2}[\ln\left(\frac{J}{J_0} \times \frac{(J_0 - J^*)}{(J - J^*)}\right) - J^*\left(\frac{1}{J} - \frac{1}{J_0}\right)] \tag{9}$$

where J_0 is the initial flux of the membrane (m/s). Since J_0 and J^* are constant, Eq. (9) can be further simplified to Eq. (10):

$$k_l t = K \tag{10}$$

where $K = 1/\ J^{*2}[\ln\left(\frac{J}{J_0} \times \frac{(J_0 - J^*)}{(J - J^*)}\right) - J^*\left(\frac{1}{J} - \frac{1}{J_0}\right)]$.

In the context of constant flux crossflow filtration, the fouling mechanisms were determined to predominantly involve intermediate pore blocking, cake filtration, or a combination of both, as proposed by Kirschner et al. [51]. The standard pore blocking and complete pore blocking models are not considered in this work since they are not realistic to result in constant flux with progressive blocking of pore opening and inner pores [51]. Eq. (11) and (12) are the models representing intermediate pore blocking and cake filtration mechanisms.

$$\Delta P = \Delta P_0 \Big/ [\frac{1}{k_i} + (1 - \frac{1}{k_i}) \times \exp(-k_i B t)] \tag{11}$$

$$\Delta P = \Delta P_0 (1 + k_l J t) \tag{12}$$

where ΔP is the transmembrane pressure (N/m^2), ΔP_0 is the initial transmembrane pressure (N/m^2), k_i and k_l are the intermediate pore blocking constant and cake filtration constant, B is particle resuspension rate (s^{-1}), J is the permeate flux (m/s), and t is the filtration time (s).

3. Results and discussion

3.1. Threshold flux determination

The results of the flux stepping experiments and the threshold fluxes of all membranes are shown in Fig. S2 and Fig. 3. The threshold fluxes of the membranes were determined using the method recommended by Kirschner et al. [44]. The pristine Al_2O_3 membrane exhibited a threshold flux of 93 L m^{-2} h^{-1}. After a deposition of a SiC layer for 60 min, the threshold flux of D60 decreased to 86 L m^{-2} h^{-1}. With a further increase in deposition time to 90 min, the threshold flux of D90 increased to 95 L m^{-2} h^{-1}. However, the threshold flux of the membrane (D120) decreased to 85 L m^{-2} h^{-1} when the deposition time was extended to 120 min. Therefore, D90 was considered to be the membrane with

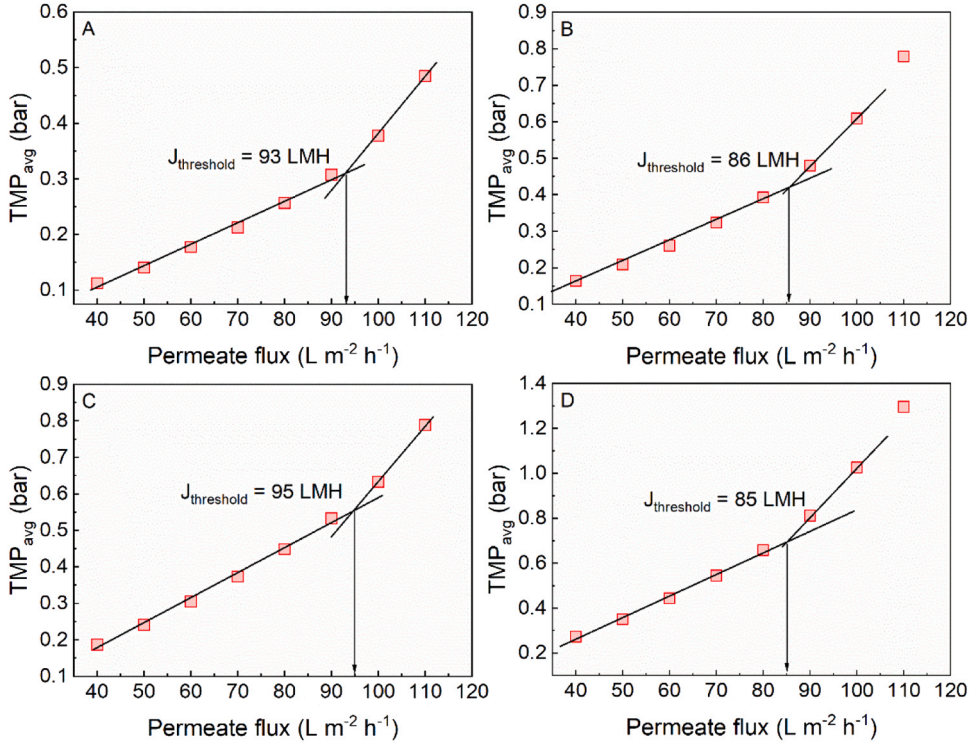

Fig. 3. Threshold flux determination from flux stepping experiment. (A) D0, (B) D60, (C) D90, and (D) D120. TMP_{avg} was calculated as the arithmetic mean of all TMPs recorded during each flux step. Based upon the slope of the TMP_{avg}/flux relationship, the data were separated into two regions. The intersection of two regression lines was identified as the threshold flux ($J_{threshold}$).

highest fouling resistance.

The morphology and surface roughness of the membranes before and after modification were investigated in our previous work [7,25]. No significant differences were observed in surface morphology or roughness among the membranes (see AFM images in Fig. S3). However, the deposition resulted in a reduced pore size and a narrower pore size distribution [25]. More importantly, the surface hydrophilicity and negative surface charge increased following the modification (Table S1 and Fig. S4, supporting information) with a greater impact on surface charge than on surface hydrophilicity as deposition time increased. For a short deposition time (60 min), the membrane (D60) was endowed with a slightly negatively charged and more hydrophilic surface. This may lead to the alleviation of membrane fouling. However, deposition also decreased the membrane pore sizes, resulting in a lower water permeance. Therefore, the membrane had to be operated at a higher pressure to maintain the same flux as the pristine membrane. The electrostatic repulsion in the D60 membrane was apparently not strong enough to compensate for the loss of water permeance, leading to a decrease in threshold flux. When the deposition time was increased to 90 min, a much higher negative charge was observed for D90 (-36.47 mV) as compared with D60 (-20 mV) (Table S1). Such a considerable increase in the zeta potential of the membrane would result in a much stronger electrostatic repulsion between the membrane surface and oil droplets [52]. In this case, apparently, the effect of electrostatic repulsion outweighed the loss of water permeance of the membrane, leading to a slightly higher threshold flux than that of the Al_2O_3 membrane. Compared with D90, a further increase in the deposition time of SiC layer had little effect on enhancing the zeta potential of the membrane (D120). However, the pore size reduction made the water permeance of the membrane even smaller (Table 1), leading to a decrease in the threshold flux again. The decrease in threshold flux, due to extensive surface modification (e.g., higher concentrations of modifying agents or longer deposition time), was also observed in the previous studies [44,45]. Kasemset et al. [45] studied the effect of polydopamine (PDA) coating on the threshold flux of hydrophobic polysulfone UF membranes. PDA is a highly hydrophilic material that enhances membrane surface hydrophilicity even at low initial concentrations or short coating times. The increased surface hydrophilicity of the membrane made it more resistant to fouling by hydrophobic oil droplets under a given shear force. A higher threshold flux was thus observed. However, at higher initial PDA concentrations or with longer coating times, the threshold flux of the modified membranes decreased due to a significant reduction in water permeance.

From the above results, it was thus concluded that the threshold fluxes of the pristine Al_2O_3 and SiC-deposited ceramic membranes were in the following order: D90 > D0 > D60 > D120.

3.2. Fouling comparison at constant flux

3.2.1. Single-cycle filtration

Constant flux crossflow single-cycle filtration was performed on alumina membrane (D0) and SiC-deposited membranes (D60, D90 and D120) using an O/W emulsion feed to evaluate differences in total fouling among the membranes. Fig. 4 presents the normalized TMP evolution as a function of filtration time at 60, 80, 90, and 100 L m^{-2} h^{-1}. These fluxes are, respectively, either below or above the threshold flux of the membranes. As shown in Fig. 4A, at 60 L m^{-2} h^{-1}, the normalized TMP of all membranes increased linearly over 1 h filtration time at a slow rate. Except for D120, the fouling curves of the other three membranes overlapped, indicating that the fouling rate was similar, which was confirmed by the UMFI values of the membranes (Fig. 4E). Since 60 L m^{-2} h^{-1} is well below the threshold flux, fouling progressed slowly, allowing the membranes to maintain relatively stable long-term operation. Similar results were also reported when using polymeric membranes for filtration O/W emulsion at fluxes below the threshold flux [44,46].

When the membranes were operated at 80 L m^{-2} h^{-1}, a distinct difference was observed as compared with the condition at 60 L m^{-2} h^{-1}. All membranes experienced a relatively constant slow increase in TMP in the first 20 min, followed by a rapid rise, indicating a substantial increase in fouling rate. The UMFI values of all membrane were also much higher than those at 60 L m^{-2} h^{-1}. Since 80 L m^{-2} h^{-1} was still below the threshold flux, a slow and constant increase of TMP was to be expected [52]. However, because the membranes were operated in a closed loop crossflow filtration system, the oil concentration increased with filtration time, probably accelerating the fouling of the membranes [53]. In addition, it can be expected that pore blockage was the main fouling mechanism during the initial slow, linear TMP increase stage [54]. To maintain the constant flux over the entire filtration area, the flux through the open pores increased, leading to fouling acceleration

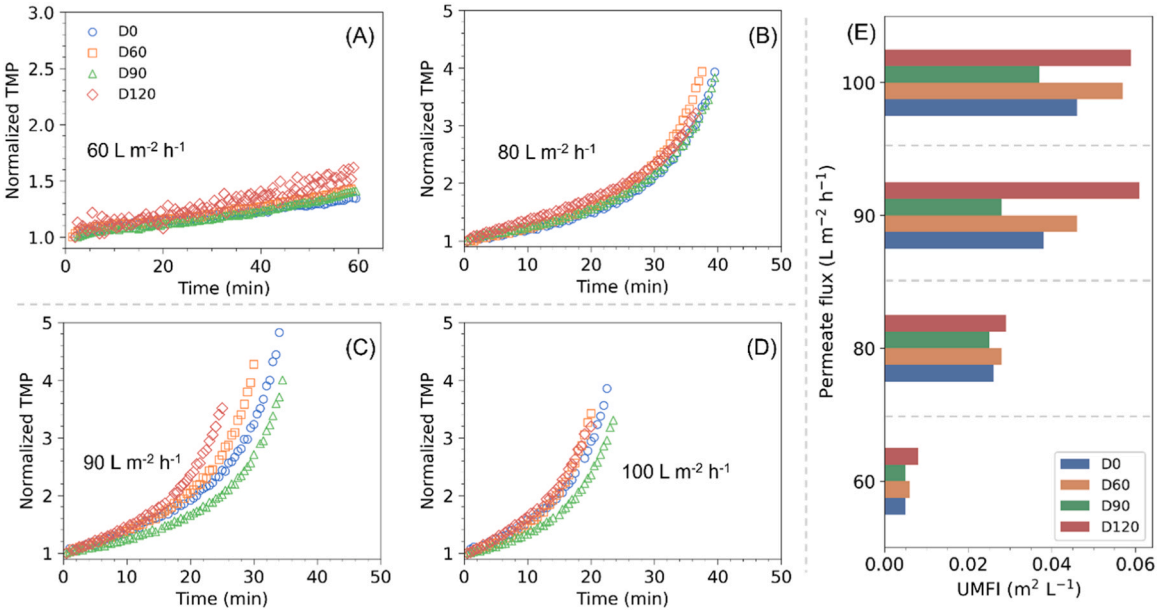

Fig. 4. Normalized TMP during constant flux fouling of Al_2O_3 and SiC-deposited ceramic membranes with O/W emulsion in single-cycle filtration experiments. (A) 60, (B), 80, (C) 90, (D) 100 L m^{-2} h^{-1} and (E) the UMFI of each membrane at the measured permeate fluxes.

[55], in this case, after 20 min.

At 90 L m^{-2} h^{-1}, the rapid increase in (normalized) TMP occurred earlier for all membranes, as expected [56]. In addition, from Fig. 4C it can be observed that the TMP increase was higher for D60 and D120, since 90 L m^{-2} h^{-1} was above their threshold flux. The lower TMP increase of D90 was attributed to its high threshold flux. The higher fouling resistance of D90 was also reflected in its UMFI values, as a much slower increase in UMFI (Fig. 4E) was observed compared to other three membranes when the flux increased from 80 to 90 L m^{-2} h^{-1}. At 100 L m^{-2} h^{-1}, a similar TMP increase order was observed except that the extent of TMP increase of D60 was close to that of D120. Overall, the extent of the TMP increase and the UMFI values in the membranes during single-cycle filtration of an O/W emulsion were consistent with their threshold flux values.

3.2.2. *Multi-cycle filtration*

Fig. 5 illustrates the permeance recovery of all membranes after each backwash during emulsion filtration at three different fluxes. A decreasing trend was observed as the number of backwash cycles increased, suggesting a gradual buildup of hydraulically irreversible fouling. Furthermore, a more pronounced decline in permeance recovery after each backwash was observed for all membranes at higher permeate fluxes. This indicates that the applied flux not only influenced the permeance decline during filtration but also affected the effectiveness of the backwash process.

At 80 L m^{-2} h^{-1} (Fig. 5A), the permeance recovery of D120 after the first backwash was a little smaller than that of the other membranes. However, with more backwash cycles, the permeance recovery of D120 considerably decreased, only reaching 85 % after the 5th backwash, while the other three membranes had a high permeance recovery of 95 %. During the single-cycle filtration experiment, the difference in fouling among all membranes was relatively small at the flux of 80 L m^{-2} h^{-1}. Therefore, the permeance recovery could be related to the backwash efficacy. Due to the inherent properties of SiC, polar interactions between the membrane surface and oil droplets were expected to be reduced. As a result, fewer oil droplets adhered to the modified membrane surfaces compared to the unmodified alumina membrane. This trend was evident for the mildly modified membranes (D60 and D90). However, despite having the most negatively charged surface, the D120 membrane exhibited lower permeance recovery after backwashing than the other membranes.

The low permeance recovery of D120 can be ascribed to its low permeance, requiring a higher transmembrane pressure (TMP) to achieve an equivalent flux as the other membranes. This elevated TMP could potentially overcome electrostatic repulsive forces, leading to increased droplet deformation and stronger adhesion to the membrane surface (Fig. 5D). Additionally, since backwashing was conducted at a constant pressure (3 bar), it was likely less effective for the less permeable membrane (D120). The gradual accumulation of foulants may have further accelerated membrane fouling by diminishing the electrostatic repulsion between the fouled surface and incoming foulants [57].

Therefore, in a multi-cycle filtration experiment, using the same backwash flux for all membranes can facilitate the comparison of their cleaning efficacy. This is because the backwash flux is the driving force that removes the cake layer from the membranes. However, the permeance of the membranes will affect the cleaning efficacy. By increasing the backwash pressure of the low permeable membranes, the backwash cleaning will be more effective for the deposited membranes, particularly D120, when the same backwash flux is used.

As shown in Fig. 5B, at 90 L m^{-2} h^{-1}, the higher permeate flux possibly caused a stronger drag force acting on the oil droplets, which consequently led to more irreversible fouling [7]. As a result, the permeance recovery of the pristine Al_2O_3 membrane (D0) was the lowest after each backwash due to the lack of electrostatic repulsion between the membrane and oil droplets. In addition, although D60 had a higher permeance than that of D90, its negative surface charge was much lower than that of D90 (Table S1). Therefore, the adsorption of negatively charged oil droplets on D90 was expected to be weaker than that of D60, leading to a higher permeance recovery during backwash [58,59].

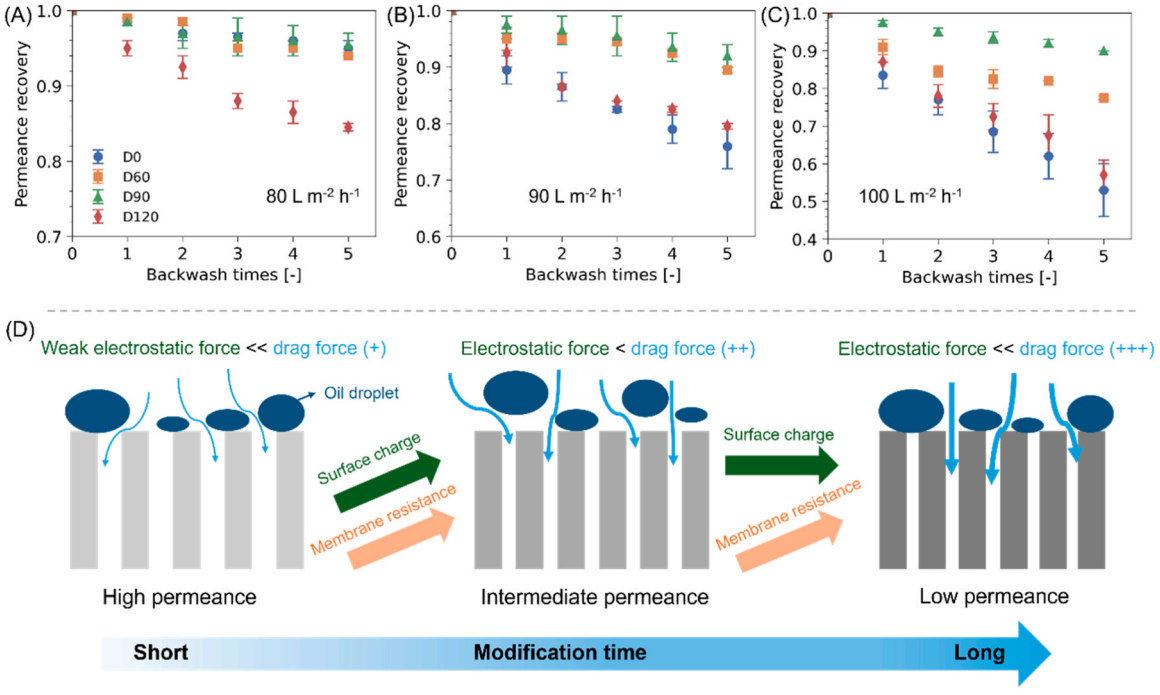

Fig. 5. Permeance recovery after each backwash during constant flux fouling of Al_2O_3 and SiC-deposited ceramic membranes with O/W emulsion at various fluxes. (A) 80 L m^{-2} h^{-1}, (B) 90 L m^{-2} h^{-1}, and (C) 100 L m^{-2} h^{-1}. (D) A schematic diagram illustrates the impact of modification time on membrane fouling due to the interactions between electrostatic forces and permeate drag force in a constant-flux filtration experiment. The error bar is calculated based on data from two filtration experiments.

Compared with D120, D90 had a higher permeance and a similar negative surface charge. As a result, the permeance recovery of D90 was higher. The higher backwash efficacy of D60 compared to D120 indicates that the effect of permeance outcompeted the influence of enhanced surface charge (Fig. 5D). According to the study by Vroman et al. [60], a critical backwash flux existed to reach a high backwash efficacy during ultrafiltration of a bentonite suspension. Above the critical backwash flux, the backwash became effective. The low backwash efficacy of D120 was probably due to the backwash flux being below the critical backwash flux.

At 100 L m^{-2} h^{-1}, the same backwash efficacies were observed as at 90 L m^{-2} h^{-1}. The permeance recovery of D90 was much higher than that of the other membranes, indicating that D90 was best resistant against fouling.

Overall, the fouling of the membranes was affected by several factors, i.e., permeate flux and membrane properties, especially when backwash was involved. Without backwash (single-cycle filtration), fouling of the membrane was mainly determined by the interactions between the membrane surface and the foulants. With backwash, however, considerable improvement on fouling control was obtained for the mildly modified membranes (D60 and D90). Similar results were reported by Ma et al. [61,62], who found that for filtration of carboxylate modified latex by membranes, fouling was not strongly dependent on the membrane surface chemistry without backpulsing. However, when backflushing was applied, the permeate volume was respectively increased by 10 % and decreased by 20 % when the modified membrane and particles had like and opposite charges, compared with the unmodified one.

3.3. Fouling comparison at constant TMP

3.3.1. Same driving force

The SiC-deposited membranes and Al_2O_3 membrane were compared at two different TMPs (0.5 and 1 bar) for O/W emulsion filtration, as shown in Fig. 6. At 0.5 bar, a flux decline was observed for D0 and D60 (Fig. 6A). In comparison, the fluxes of D90 and D120 did not change with the filtration time, indicating that no fouling occurred in these membranes. When a constant TMP (0.5 bar) was applied, D0 exhibited the highest initial flux, reaching up to 150 L m^{-2} h^{-1}. This flux was significantly higher than the threshold flux of D0 and likely led to the development of both reversible and irreversible fouling (internal pore blocking). The initial flux of D60 was approximately 100 L m^{-2} h^{-1}, also exceeding its threshold flux. However, unlike D0, the flux of D60 was almost fully recovered after backwashing, indicating that the fouling was primarily hydraulically reversible. The initial fluxes of D90 and D120 were around 70 and 60 L m^{-2} h^{-1}, which were well below the threshold fluxes of the membranes. As a result, the fouling hardly built up on the membrane surface.

At 1 bar, flux declines of all membranes were observed. The initial fluxes of all membranes were higher than their threshold fluxes, as depicted in Fig. 6B. Due to its higher initial flux, the flux decline of D0 was much higher than the decline of the other three membranes. As the fouling curves of the SiC-deposited ceramic membranes overlapped (Fig. 6B), the normalized flux was presented in Fig. 6C, to better illustrate the fouling and flux recovery of the membranes. As shown, D120 had the smallest flux decline and the highest flux recovery, followed by D90, D60 and D0. This suggests that the less permeable membranes exhibited higher flux recovery and experienced less fouling, regardless of their surface properties. For membranes with higher permeability, internal pore blocking may occur more readily due to the higher initial flux. However, it should be noted that under constant TMP conditions, membranes with lower permeance also produced less permeate. Consequently, the reduced fouling observed in these membranes may be partly attributed to their lower throughput [28]. Comparison at the constant TMPs with a similar initial flux is thus needed to have a better assessment of the membrane fouling.

3.3.2. Equal initial fluxes at constant TMP

Fig. 7 illustrates the permeance recovery of membranes after each backwash based on equal initial fluxes (167–175 L m^{-2} h^{-1}) (Table S2)

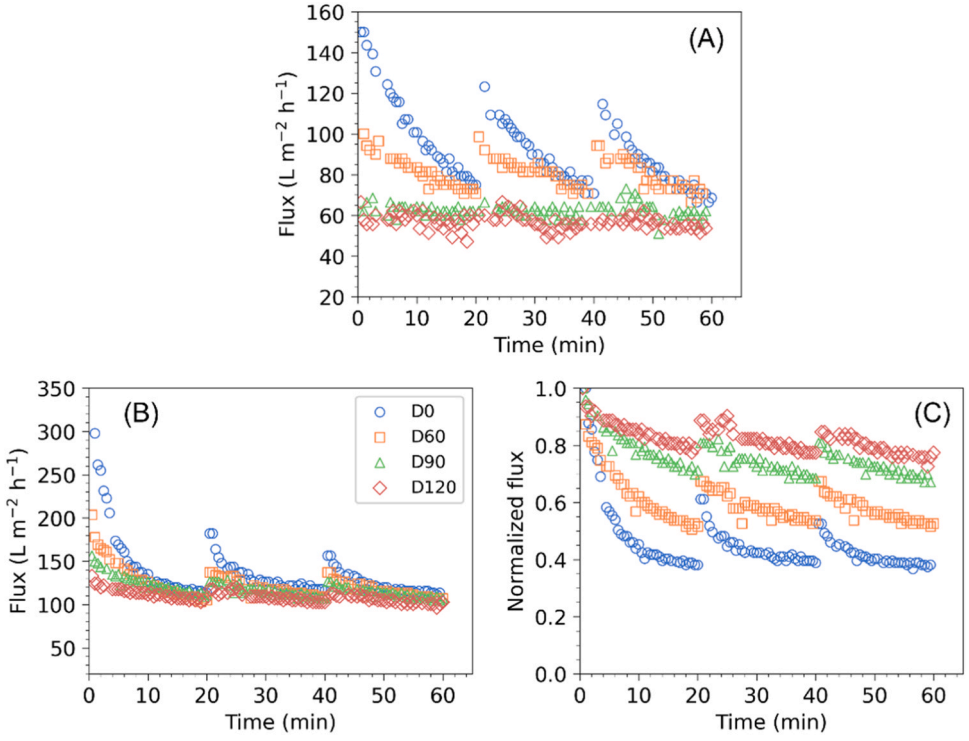

Fig. 6. Time-dependent variations of permeate flux of Al_2O_3 and SiC-deposited ceramic membranes for O/W emulsion filtration with three cycles. (A) 0.5 bar, (B) 1 bar, (C) normalized flux at 1 bar. The normalized flux was calculated based on the ratio of permeate flux to the initial permeate flux of each membrane.

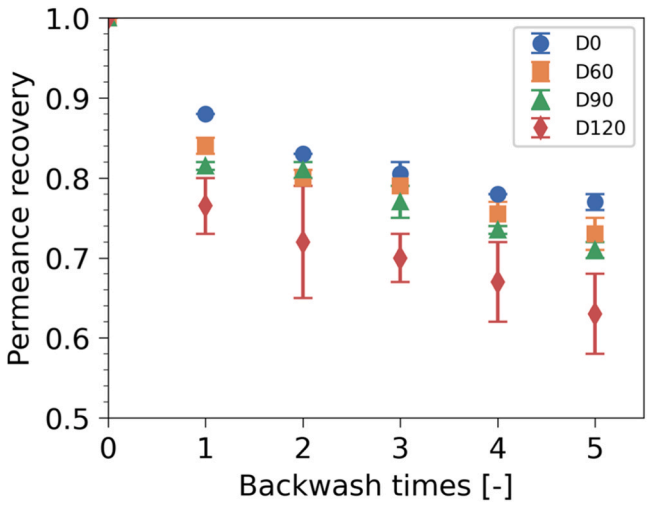

Fig. 7. Permeance recovery during constant pressure O/W emulsion filtration with Al_2O_3 and SiC-deposited ceramic membranes at similar initial fluxes. The error bar is calculated based on data from two filtration experiments.

at constant TMP. In contrast to the results observed under the same driving forces, D0 exhibited the highest flux recovery among the membranes, followed by D60, D90, and D120. One possible explanation for this phenomenon is that the applied initial flux was significantly higher than the threshold flux for all membranes, leading to similar fouling accumulation during the filtration process. Membranes with higher permeance, such as D0, experienced higher cleaning efficacy due to its higher backwash flux. This suggests that the pristine membrane performed best in terms of fouling resistance. While this might imply that modification does not significantly alleviate fouling, it contradicts the conclusions drawn under constant flux filtration conditions.

On the other hand, when membranes were compared at similar initial fluxes, higher TMPs were required for the less permeable membranes. Unlike rigid particles, oil droplets are deformable. Oil deformation is expected to be higher at higher pressures [63]. The deformation of oil droplets on the membrane surface may lead to a stronger attachment or facilitate their entry into the pores, making them even harder to remove during backwashing. Evidence of oil fouling within the membrane pores will be further analysed using fouling models in Section 3.5.

3.4. Membrane rejection

For all fouling experiments, including both constant flux and constant TMP filtration, all membranes exhibited a high oil rejection (> 98 %) due to their smaller pore size compared to the oil droplet size (Fig. 8). In constant flux filtration, an increase in oil rejection was observed for the membranes with increased permeate flux, which could be ascribed to the enhanced concentration polarization on the membrane surface [29]. For constant TMP fouling, modified membranes demonstrated a higher oil rejection than the pristine alumina membranes at a TMP of 0.5 bar due to their smaller pore size and enhanced electrostatic repulsion between the membrane and oil droplets after modification. However, when the TMP was increased from 0.5 to 1 bar, a slight decline in oil rejection has been observed for all membranes,

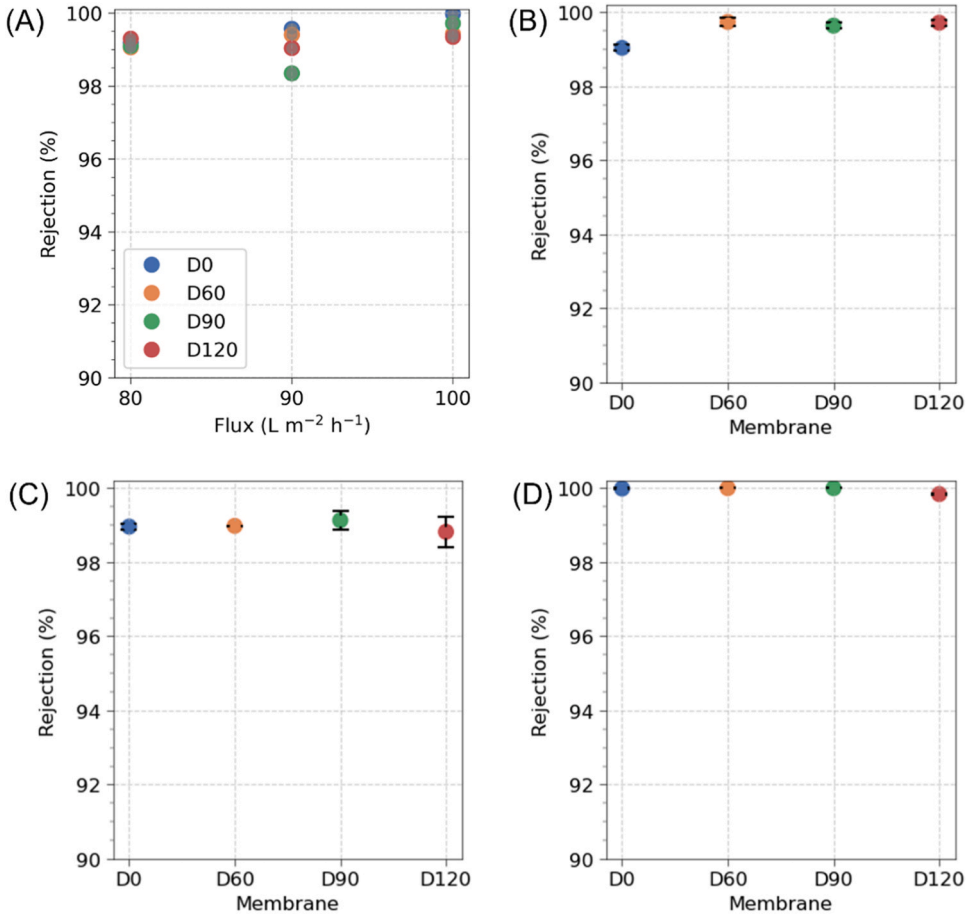

Fig. 8. Oil rejection at constant flux and constant TMP conditions. (A) oil rejection at three different fluxes in constant flux filtration, and oil rejection in constant TMP filtration at (B) 0.5 bar, (C) 1 bar and (D) equal initial flux. The error bar is calculated based on the multicycle experiments.

possibly due to the higher permeate drag force at higher pressure. Under constant TMP conditions, when an equal initial flux was applied, all membranes achieved high oil rejection (>99 %).

3.5. Fouling mechanism analysis at constant flux and constant TMP filtration conditions

Fouling on a membrane surface is assumed to begin with a pore blocking process followed by cake layer formation. However, three distinct pore blocking mechanisms are typically observed in membrane fouling. The primary fouling mechanism of the membrane can be identified by fitting the experimental data to the models developed, as described in Section 2.8.

For constant TMP filtration, four different fouling models were respectively fitted to the experimental data from Fig. 7. As depicted in Fig. 9, the standard pore blocking and complete pore blocking models demonstrated a superior fitting to the experimental data, in comparison to the cake layer and intermediate pore blocking models. This observation is substantiated by the higher correlation coefficients for these models when aligned with the experimental data. For example, the fitting of both the standard pore blocking and complete pore blocking with D60 gave the highest R^2 of 0.96, followed by intermediate pore blocking model ($R^2 = 0.92$) (Table 3). Similar results were observed for the other three membranes. As a result, it is highly probable that internal pore blocking occurred in the initial stages of the membrane fouling during constant TMP filtration. At a later stage, the membrane pores became completely blocked by oil droplets. Due to the relatively short filtration time, a cake layer had not yet formed on the membrane surface. To determine the optimal fouling model, an Akaike Information Criterion (AIC) analysis was conducted for sample D60. The complete pore blocking model yielded the lowest AIC value (-930.84), followed by the standard pore blocking model (-929.96) and the intermediate pore blocking model (-906.25). A lower AIC value indicates a better fit, suggesting that the complete pore blocking and internal blocking models best describe the fouling behavior under constant TMP conditions in this study.

Regarding the fouling constant (k value), no significant differences were observed among the samples across all fouling models. This further supports the importance of backwashing in permeance recovery. Membranes with higher permeance demonstrated better cleaning efficiency, likely due to a higher backwash flux.

In contrast, the pore blocking mechanism for constant flux filtration can be well explained by the intermediate pore blocking model. As shown in Fig. 10, the fitting of intermediate pore blocking with the experimental data of D60 was superior, giving a R^2 of 0.95. The remaining three membranes also exhibited satisfactory fitting results when analyzed using the intermediate pore blocking model (Table 4). In addition, the fouling kinetics, indicative of the interactions between the membrane and oil droplets, are reflected from the intermediate pore blocking constant (k value). A higher k value indicates more rapid

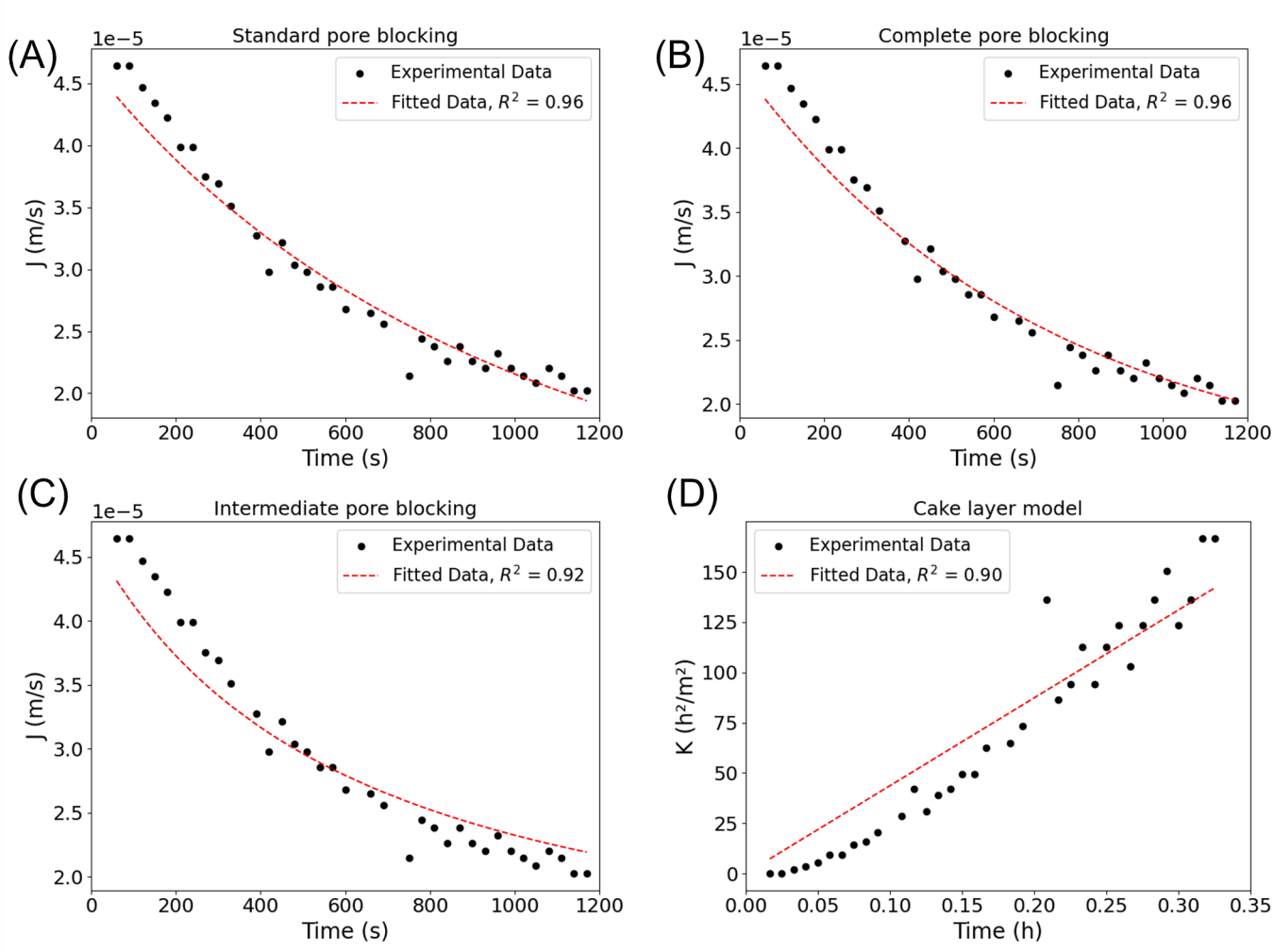

Fig. 9. Modelling of oil droplets fouling mechanism at constant TMP conditions. (A) standard pore blocking, (B) complete pore blocking, (C) intermediate pore blocking and (D) cake layer filtration. The experimental data here used for modelling are from D60 in Fig. 7. $J^* = 50$ L m^{-2} h^{-1} was used for model fitting.

Table 3
Fitting parameters of fouling models at constant TMP filtration condition, the data used for fitting are from Fig. 7.

Sample	Standard pore blocking		Complete pore blocking		Intermediate pore blocking		Cake layer	
	k_s (m^{-1})	R^2	k_c (s^{-1})	R^2	k_i (m^{-1})	R^2	k_l ($s{\cdot}m^{-2}$)	R^2
D0	0.056	0.96	0.0011	0.96	29.42	0.94	0.06	0.92
D60	0.069	0.96	0.0014	0.96	39.99	0.92	0.12	0.90
D90	0.058	0.97	0.0011	0.97	30.57	0.95	0.06	0.94
D120	0.068	0.98	0.0013	0.98	38.02	0.96	0.10	0.94

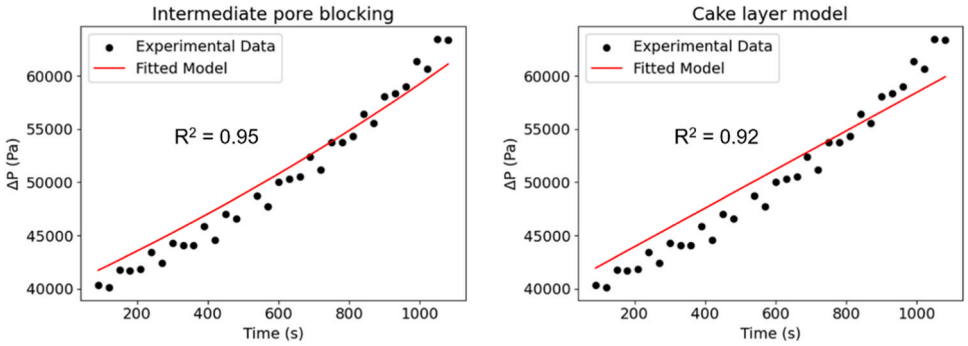

Fig. 10. Modelling of oil droplets fouling mechanism at constant flux conditions with intermediate pore blocking (left) and cake layer models (right). The experimental data here used for modelling are from D60 in Fig. 5C.

Table 4
Fitting parameters of fouling models at constant flux filtration condition, the data used for fitting are from Fig. 5C.

Sample	Intermediate pore blocking			Cake layer	
	k_i (dimensionless)	B (s^{-1})	R^2	k_l (m^{-1})	R^2
D0	222.41	2.37×10^{-6}	0.94	23.39	0.88
D60	179.65	2.16×10^{-6}	0.95	16.21	0.92
D90	150.88	1.88×10^{-6}	0.97	11.37	0.96
D120	212.45	2.32×10^{-6}	0.98	21.76	0.96

fouling on the membrane surface and vice versa. As shown in Table 4, D90 had the lowest k value, succeeded by D60, D120 and D0, which is consistent with the flux recovery observations in Fig. 5C. Therefore, we can assume that the internal pore blocking is less likely to happen in constant flux filtration experiments, with intermediate pore blocking being the predominant fouling mechanism in the initial stage.

Based on the discussions above, the fouling mechanisms for constant TMP and constant flux filtrations have been identified and are schematically illustrated in Fig. 11. For constant TMP filtration, standard pore blocking and complete pore blocking are the primary mechanisms, while intermediate pore blocking accompanied by cake filtration aptly describes the fouling observed in constant flux experiments. During constant TMP filtration, high initial membrane flux tends to draw oil droplets into the pores, increasing the probability of internal pore blocking. Such blockages are challenging to remove during backwashing, leading to lower flux recovery. Additionally, when oil droplets are trapped within membrane pores, the membrane's surface charge has a negligible effect. Conversely, in constant flux filtration, intermediate pore blocking predominates due to the lower flux used, with the membrane's surface charge and hydrophilicity playing a significant role in fouling, especially since the surfactant-stabilized hydrophobic oil droplets carry the same charge as the membrane.

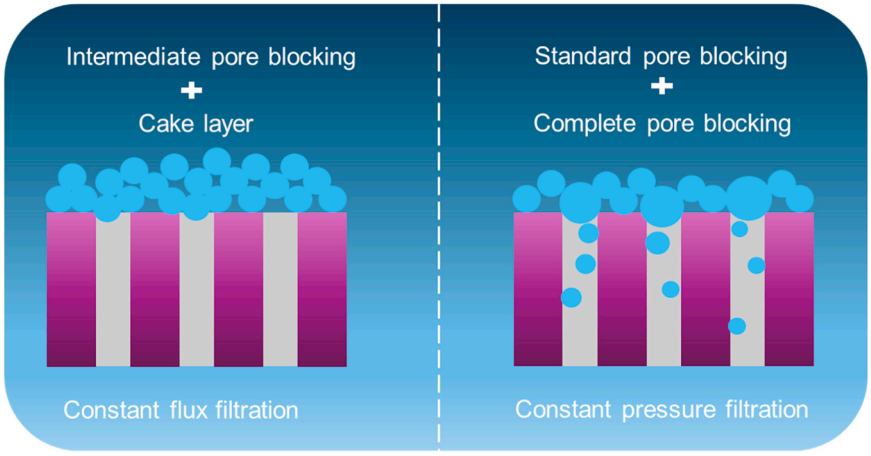

Fig. 11. Schematic representation of fouling mechanisms in constant flux and constant TMP filtration conditions. Standard pore blocking and complete pore blocking are the main fouling mechanism in constant TMP filtration, while intermediate pore blocking, and cake layer filtration are responsible for membrane fouling in constant flux filtration.

3.6. Implications for membrane modification

Membrane modification has been widely used to improve membrane rejection and/or to develop fouling resistant membranes for water treatment, especially for O/W emulsions. In some cases, the trade-off between the membrane selectivity and permeability may be overcome by coating a highly hydrophilic thin layer on the membrane support [64, 65]. Still, the decrease in pure water permeance of the modified membrane is a common phenomenon [25,46]. To evaluate the fouling resistance, a constant TMP filtration system is generally applied at a laboratory scale. However, the results found in this work suggest that the effect of permeance of the membranes seems to be dominant in this filtration mode. The backwash efficacy was only related to the permeance of membranes, while an effect of surface properties was not observed. The improved fouling resistance of the membrane after modification could be attributed to the huge loss in permeance, thereby resulting in a much lower initial flux and fouling when operated at the same driving force as the pristine membrane. However, in constant flux filtration experiments, we found that the loss of water permeance of the membranes after modification may lead to negative effects on fouling resistance even though the surface property of membranes became less prone to the target pollutants. Apparently, these two filtration modes give different conclusions on the performance of the modified ceramic membranes for the O/W emulsions filtration. In constant TMP experiments, the best-performing modified membranes are those with either the lowest or highest permeance, which may not necessarily represent optimal choices in practical applications. In contrast, constant flux experiments more clearly reveal the competing effects between membrane permeance and the enhanced fouling resistance provided by the coating layer. Moreover, this setup offers a more realistic simulation of practical O/W emulsion filtration conditions. In addition, due to the high initial flux of the clean membrane, severe fouling (internal pore blocking) often occurs at the start of the constant TMP experiment. This could be prevented by imposing a lower flux in constant flux filtration [29]. Therefore, constant flux filtration experiments with backwash are recommended to be applied to evaluate the performance of the membranes with and without modification for O/W filtration as well as other types of wastewater treatment. As the height of permeate flux can also affect the order of fouling tendency, experiments tested at several permeate fluxes would be preferred.

4. Conclusion

The performance of alumina and SiC-deposited ceramic membranes was respectively compared at constant flux and constant TMP filtration modes with O/W emulsions in order to evaluate its practical applicability. The filtration conditions (filtration modes, permeate flux and TMP), membrane properties and the backwash affected the fouling of the membranes. The following conclusions were drawn:

- During single-cycle constant flux filtration experiments, it was difficult to make a distinction between the fouling of the membranes when the permeate flux was low (60 and 80 L m^{-2} h^{-1}). At higher permeate flux (90 and 100 L m^{-2} h^{-1}), the fouling of the modified membranes D90 was lowest, followed by D0, D60 and D120.
- When backwash was involved in constant flux filtration mode, except for D120, hardly any difference in irreversible fouling was observed at a low flux (80 L m^{-2} h^{-1}). At higher fluxes (90 and 100 L m^{-2} h^{-1}), two of the three modified membranes (D90 and D60 respectively) performed better, in terms of irreversible fouling, than the pristine membrane, indicating the importance of incorporating backwash in a fouling experiment for good evaluation.
- During the constant TMP filtration experiments, membrane fouling was observed to be only related to the membrane permeance, while an effect of surface properties was not observed.
- Standard pore blocking and complete pore blocking were the main fouling mechanism for constant TMP filtration experiments, while intermediate pore blocking and cake layer filtration were more likely to happen in constant flux filtration.
- Since it is also the case in operation of a full-scale MF/UF plant, experiments with constant flux filtration with backwash were considered to be the most suitable for irreversible membrane fouling comparison, as compared with constant TMP filtration or experiments without backwash, leading to erratic conclusions.

CRediT authorship contribution statement

Luuk C. Rietveld: Writing – review & editing, Supervision. **Mingliang Chen:** Writing – original draft, Visualization, Validation, Data curation, Conceptualization. **Sebastiaan G.J. Heijman:** Writing – review & editing, Supervision.

Declaration of Competing Interest

The authors declare that they have no known competing financial interests or personal relationships that could have appeared to influence the work reported in this paper.

Acknowledgements

Mingliang Chen acknowledges the China Scholarship Council for his Ph.D. scholarship under the State Scholarship Fund (No. 201704910894). We thank WaterLab at TU Delft for providing the help on the measurement of samples. Bob Siemerink, and Iske Achterhuis from Twente University are acknowledged for the support concerning the zeta potential measurements.

Appendix A. Supporting information

Supplementary data associated with this article can be found in the online version at doi:10.1016/j.jece.2025.117823.

Data availability

Data will be made available on request.

References

[1] L. Fiksdal, T. Leiknes, The effect of coagulation with MF/UF membrane filtration for the removal of virus in drinking water, J. Membr. Sci. 279 (2006) 364–371.
[2] V. Mavrov, H. Chmiel, J. Kluth, J. Meier, F. Heinrich, P. Ames, K. Backes, P. Usner, Comparative study of different MF and UF membranes for drinking water production, Desalination 117 (1998) 189–196.
[3] M. Raffin, E. Germain, S. Judd, Wastewater polishing using membrane technology: a review of existing installations, Environ. Technol. 34 (2013) 617–627.
[4] J. Hoinkis, S.A. Deowan, V. Panten, A. Figoli, R.R. Huang, E. Drioli, Membrane bioreactor (MBR) technology–a promising approach for industrial water reuse, Procedia Eng. 33 (2012) 234–241.
[5] R. Ordóñez, D. Hermosilla, I. San Pío, Á. Blanco, Evaluation of MF and UF as pretreatments prior to RO applied to reclaim municipal wastewater for freshwater substitution in a paper mill: a practical experience, Chem. Eng. J. 166 (2011) 88–98.
[6] G.K. Pearce, UF/MF pre-treatment to RO in seawater and wastewater reuse applications: a comparison of energy costs, Desalination 222 (2008) 66–73.
[7] M. Chen, S.G.J. Heijman, M.W.J. Luiten-Olieman, L.C. Rietveld, Oil-in-water emulsion separation: fouling of alumina membranes with and without a silicon carbide deposition in constant flux filtration mode, Water Res. 216 (2022) 118267.
[8] M. Chen, S.G.J. Heijman, L.C. Rietveld, State-of-the-art ceramic membranes for oily wastewater treatment: modification and application, Membranes 11 (2021) 888.
[9] M. Chen, L. Zhu, J. Chen, F. Yang, C.Y. Tang, M.D. Guiver, Y. Dong, Spinel-based ceramic membranes coupling solid sludge recycling with oily wastewater treatment, Water Res. 169 (2020) 115180.
[10] M.L. Chen, L. Zhu, Y.C. Dong, L.L. Li, J. Liu, Waste-to-Resource Strategy To Fabricate Highly Porous Whisker-Structured Mullite Ceramic Membrane for Simulated Oil-in-Water Emulsion Wastewater Treatment, ACS Sustain. Chem. Eng. 4 (2016) 2098–2106.

[11] D. Zou, M. Qiu, X. Chen, E. Drioli, Y. Fan, One step co-sintering process for low-cost fly ash based ceramic microfiltration membrane in oil-in-water emulsion treatment, Sep. Purif. Technol. 210 (2019) 511–520.
[12] M. Chen, S.G.J. Heijman, L.C. Rietveld, Ceramic membrane filtration for oily wastewater treatment: basics, membrane fouling and fouling control, Desalination 583 (2024) 117727.
[13] N. Zhang, X. Yang, Y. Wang, Y. Qi, Y. Zhang, J. Luo, P. Cui, W. Jiang, A review on oil/water emulsion separation membrane material, J. Environ. Chem. Eng. 10 (2022) 107257.
[14] P.D. Sutrisna, K.A. Kurnia, U.W.R. Siagian, S. Ismadji, I.G. Wenten, Membrane fouling and fouling mitigation in oil–water separation: a review, J. Environ. Chem. Eng. 10 (2022) 107532.
[15] P.D. Sutrisna, K. Khoiruddin, P.C.W.B. Mustika, S. Ismadji, I.G. Wenten, Advancements in ceramic membranes for robust oil-water separation, J. Environ. Chem. Eng. 12 (2024) 113658.
[16] D.J. Miller, D.R. Dreyer, C.W. Bielawski, D.R. Paul, B.D. Freeman, Surface modification of water purification membranes, Angew. Chem. Int. Ed. 56 (2017) 4662–4711.
[17] R. Zhang, Y. Liu, M. He, Y. Su, X. Zhao, M. Elimelech, Z. Jiang, Antifouling membranes for sustainable water purification: strategies and mechanisms, Chem. Soc. Rev. 45 (2016) 5888–5924.
[18] J. Wu, F. Chen, X. Huang, W. Geng, X. Wen, Using inorganic coagulants to control membrane fouling in a submerged membrane bioreactor, Desalination 197 (2006) 124–136.
[19] L. Heng, Y. Yanling, G. Weijia, L. Xing, L. Guibai, Effect of pretreatment by permanganate/chlorine on algae fouling control for ultrafiltration (UF) membrane system, Desalination 222 (2008) 74–80.
[20] T. Lin, S. Pan, W. Chen, S. Bin, Role of pre-oxidation, using potassium permanganate, for mitigating membrane fouling by natural organic matter in an ultrafiltration system, Chem. Eng. J. 223 (2013) 487–496.
[21] Q.B. Chang, J.E. Zhou, Y.Q. Wang, J. Liang, X.Z. Zhang, S. Cerneaux, X. Wang, Z. W. Zhu, Y.C. Dong, Application of ceramic microfiltration membrane modified by nano-TiO_2 coating in separation of a stable oil-in-water emulsion, J. Membr. Sci. 456 (2014) 128–133.
[22] L. Zhu, M.L. Chen, Y.C. Dong, C.Y. Tang, A.S. Huang, L.L. Li, A low-cost mullite-titania composite ceramic hollow fiber microfiltration membrane for highly efficient separation of oil-in-water emulsion, Water Res. 90 (2016) 277–285.
[23] N. Nady, M.C.R. Franssen, H. Zuilhof, M.S.M. Eldin, R. Boom, K. Schroën, Modification methods for poly(arylsulfone) membranes: a mini-review focusing on surface modification, Desalination 275 (2011) 1–9.
[24] Q. Zhang, Y. Fan, N. Xu, Effect of the surface properties on filtration performance of Al_2O_3–TiO_2 composite membrane, Sep. Purif. Technol. 66 (2009) 306–312.
[25] M. Chen, R. Shang, P.M. Sberna, M.W.J. Luiten-Olieman, L.C. Rietveld, S.G. J. Heijman, Highly permeable silicon carbide-alumina ultrafiltration membranes for oil-in-water filtration produced with low-pressure chemical vapor deposition, Sep. Purif. Technol. 253 (2020) 117496.
[26] D. Rana, T. Matsuura, Surface modifications for antifouling membranes, Chem. Rev. 110 (2010) 2448–2471.
[27] Q. Gu, T. Chiang Albert Ng, Y. Bao, H. Yong Ng, S. Ching Tan, J. Wang, Developing better ceramic membranes for water and wastewater treatment: where microstructure integrates with chemistry and functionalities, Chem. Eng. J. (2021) 130456.
[28] B. Blankert, B. Van der Bruggen, A.E. Childress, N. Ghaffour, J.S. Vrouwenvelder, Potential pitfalls in membrane fouling evaluation: merits of data representation as resistance instead of flux decline in membrane filtration, Membranes 11 (2021) 460.
[29] D.J. Miller, S. Kasemset, D.R. Paul, B.D. Freeman, Comparison of membrane fouling at constant flux and constant transmembrane pressure conditions, J. Membr. Sci. 454 (2014) 505–515.
[30] A. Kouchaki Shalmani, I.M.A. ElSherbiny, S. Panglisch, Application-oriented mini-plant experiments using non-conventional model foulants to evaluate new hollow fiber membrane materials, Sep. Purif. Technol. 251 (2020) 117345.
[31] K. Kimura, K. Tanaka, Y. Watanabe, Microfiltration of different surface waters with/without coagulation: clear correlations between membrane fouling and hydrophilic biopolymers, Water Res. 49 (2014) 434–443.
[32] K. Kimura, Y. Hane, Y. Watanabe, G. Amy, N. Ohkuma, Irreversible membrane fouling during ultrafiltration of surface water, Water Res. 38 (2004) 3431–3441.
[33] M. Mansha, B. Salhi, S. Ali, S.A. Khan, N. Baig, Novel procaine-based gemini zwitterion incorporated PVDF membranes for efficient treatment of oily wastewater, J. Environ. Chem. Eng. 10 (2022) 107935.
[34] N. Baig, A.M. Alowaid, I. Abdulazeez, B. Salhi, M. Sajid, I. Kammakakam, Designing of nanotextured inorganic-organic hybrid PVDF membrane for efficient separation of the oil-in-water emulsions, Chemosphere 308 (2022) 136531.
[35] N.F.H. Alrasheedi, I. Abdulazeez, N. Baig, B. Salhi, H.A. Asmaly, S.A. Haladu, A. M. Elsharif, Antifouling macrocyclic-engineered PVDF membrane for the low-pressure separation of surfactant-stabilized oily wastewater, J. Environ. Chem. Eng. 12 (2024) 112850.
[36] B. Salhi, N. Baig, I. Abdulazeez, A. Al-Ahmed, I.H. Aljundi, High flux polyaniline-coated ceramic membrane for effective separation of emulsified oil-in-water, Ceram. Int. 48 (2022) 25246–25253.
[37] N. Baig, N.A. Khan, B. Salhi, I. Abdulazeez, N. Abu-Zahra, S. Abdelazem, I. H. Aljundi, Highly permeable sulfonated polydopamine integrated MXene membranes for efficient surfactant-stabilized oil-in-water separation, Langmuir 39 (2023) 13953–13967.
[38] X. Xue, Z. Liang, J. Zhou, H. Zhang, Q. Gu, Z. Zhong, W. Xing, Tubular SiC membranes in brine purification: effects of operational parameters towards low energy consumption process, Sep. Purif. Technol. 366 (2025) 132736.
[39] J. Wang, Y. Yang, L. Zhou, F. Hu, P. Wang, W. Xin, F. Yu, S. Li, High-purity SiC ultrafiltration membrane with triple-layer asymmetric structures constructed from multiscale SiC powders, J. Eur. Ceram. Soc. 45 (2025) 117204.
[40] A.S. Romero, M.D.M. Innocentini, J. Vladimir Oliveira, A. Lider, T. Fey, N. Travitzky, D. Hotza, Unveiling the potential of silicon carbide as a support material and membranes for oily wastewater remediation, Sep. Purif. Technol. 354 (2025) 129044.
[41] M. Xu, C. Xu, K.P. Rakesh, Y. Cui, J. Yin, C. Chen, S. Wang, B. Chen, L. Zhu, Hydrophilic SiC hollow fiber membranes for low fouling separation of oil-in-water emulsions with high flux, RSC Adv. 10 (2020) 4832–4839.
[42] B. Skibinski, P. Müller, W. Uhl, Rejection of submicron sized particles from swimming pool water by a monolithic SiC microfiltration membrane: relevance of steric and electrostatic interactions, J. Membr. Sci. 499 (2016) 92–104.
[43] H. Nagasawa, T. Omura, T. Asai, M. Kanezashi, T. Tsuru, Filtration of surfactant-stabilized oil-in-water emulsions with porous ceramic membranes: effects of membrane pore size and surface charge on fouling behavior, J. Membr. Sci. 610 (2020) 118210.
[44] A.Y. Kirschner, C.-C. Chang, S. Kasemset, T. Emrick, B.D. Freeman, Fouling-resistant ultrafiltration membranes prepared via co-deposition of dopamine/zwitterion composite coatings, J. Membr. Sci. 541 (2017) 300–311.
[45] S. Kasemset, Z. He, D.J. Miller, B.D. Freeman, M.M. Sharma, Effect of polydopamine deposition conditions on polysulfone ultrafiltration membrane properties and threshold flux during oil/water emulsion filtration, Polymer 97 (2016) 247–257.
[46] D.J. Miller, S. Kasemset, L. Wang, D.R. Paul, B.D. Freeman, Constant flux crossflow filtration evaluation of surface-modified fouling-resistant membranes, J. Membr. Sci. 452 (2014) 171–183.
[47] M.C. Fraga, S. Sanches, J.G. Crespo, V.J. Pereira, Assessment of a new silicon carbide tubular honeycomb membrane for treatment of olive mill wastewaters, Membranes 7 (2017).
[48] T. Zsirai, H. Qiblawey, P. Buzatu, M. Al-Marri, S.J. Judd, Cleaning of ceramic membranes for produced water filtration, J. Petrol. Sci. Eng. 166 (2018) 283–289.
[49] H. Huang, T. Young, J.G. Jacangelo, Novel approach for the analysis of bench-scale, low pressure membrane fouling in water treatment, J. Membr. Sci. 334 (2009) 1–8.
[50] R.W. Field, D. Wu, J.A. Howell, B.B. Gupta, Critical flux concept for microfiltration fouling, J. Membr. Sci. 100 (1995) 259–272.
[51] A.Y. Kirschner, Y.-H. Cheng, D.R. Paul, R.W. Field, B.D. Freeman, Fouling mechanisms in constant flux crossflow ultrafiltration, J. Membr. Sci. 574 (2019) 65–75.
[52] Z. He, D.J. Miller, S. Kasemset, L. Wang, D.R. Paul, B.D. Freeman, Fouling propensity of a poly(vinylidene fluoride) microfiltration membrane to several model oil/water emulsions, J. Membr. Sci. 514 (2016) 659–670.
[53] Q. Yang, J. Luo, S. Guo, X. Hang, X. Chen, Y. Wan, Threshold flux in concentration mode: fouling control during clarification of molasses by ultrafiltration, J. Membr. Sci. 586 (2019) 130–139.
[54] C.-C. Ho, A.L. Zydney, Transmembrane pressure profiles during constant flux microfiltration of bovine serum albumin, J. Membr. Sci. 209 (2002) 363–377.
[55] S. Ognier, C. Wisniewski, A. Grasmick, Membrane bioreactor fouling in sub-critical filtration conditions: a local critical flux concept, J. Membr. Sci. 229 (2004) 171–177.
[56] X.B. Zhu, A. Dudchenko, X.T. Gu, D. Jassby, Surfactant-stabilized oil separation from water using ultrafiltration and nanofiltration, J. Membr. Sci. 529 (2017) 159–169.
[57] S. Hube, J. Wang, L.N. Sim, D. Ólafsdóttir, T.H. Chong, B. Wu, Fouling and mitigation mechanisms during direct microfiltration and ultrafiltration of primary wastewater, J. Water Process. Eng. 44 (2021) 102331.
[58] H. Chang, F. Qu, B. Liu, H. Yu, K. Li, S. Shao, G. Li, H. Liang, Hydraulic irreversibility of ultrafiltration membrane fouling by humic acid: effects of membrane properties and backwash water composition, J. Membr. Sci. 493 (2015) 723–733.
[59] H. Chang, H. Liang, F. Qu, B. Liu, H. Yu, X. Du, G. Li, S.A. Snyder, Hydraulic backwashing for low-pressure membranes in drinking water treatment: a review, J. Membr. Sci. 540 (2017) 362–380.
[60] T. Vroman, F. Beaume, V. Armanges, E. Gout, J.-C. Remigy, Critical backwash flux for high backwash efficiency: use of ultrafiltration of bentonite suspensions, J. Membr. Sci. (2020) 118836.
[61] H. Ma, L.F. Hakim, C.N. Bowman, R.H. Davis, Factors affecting membrane fouling reduction by surface modification and backpulsing, J. Membr. Sci. 189 (2001) 255–270.
[62] H. Ma, C.N. Bowman, R.H. Davis, Membrane fouling reduction by backpulsing and surface modification, J. Membr. Sci. 173 (2000) 191–200.
[63] T. Darvishzadeh, N.V. Priezjev, Effects of crossflow velocity and transmembrane pressure on microfiltration of oil-in-water emulsions, J. Membr. Sci. 423 (2012) 468–476.
[64] G. Mahmodi, A. Ronte, S. Dangwal, P. Wagle, E. Echeverria, B. Sengupta, V. Vatanpour, D.N. Mcllroy, J.D. Ramsey, S.-J. Kim, Improving antifouling property of alumina microfiltration membranes by using atomic layer deposition technique for produced water treatment, Desalination 523 (2022) 115400.
[65] Q. Wang, X. Wang, Z. Wang, J. Huang, Y. Wang, PVDF membranes with simultaneously enhanced permeability and selectivity by breaking the tradeoff effect via atomic layer deposition of TiO_2, J. Membr. Sci. 442 (2013) 57–64.